Climate Dynamics
https://doi.org/10.1007/s00382-022-06415-w

# Synoptic–dynamic indicators associated with blocking events over the Southeastern Pacific and South Atlantic oceans

**Monica Cristina Damião Mendes**[1,2] · **Maria Regina da Silva Aragão**[1] · **David Mendes**[2] · **Michel D. S. Mesquita**[3] · **Magaly de Fatima Correia**[1] · **Enilson Palmeira Cavalcanti**[1]

Received: 5 May 2021 / Accepted: 4 July 2022


**Abstract**
The presence of atmospheric blocking over the Southern Hemisphere causes a change in the zonal flow, resulting in the interruption of the propagation of synoptic systems. This behavior significantly affects the weather on the South American continent and adjacent oceanic areas. This work analyzes the synoptic–dynamic features of blocking, considering the atmospheric conditions that favor onset and decay days of blockings. Blocking events are identified using two meridional gradients of the geopotential height at 500 hPa, over the Southeastern Pacific (SEP) and South Atlantic (SAT) areas, for the period from 1979 to 2015. In general, during the 37 years, blocking events in SAT (SEP) are dominated by the Omega (dipole)-type pattern. Positive anomalies of potential vorticity at 200 hPa, relative vorticity at 200–850 hPa and geopotential height at 500 hPa are found near the blocking regions, two days before onset ($[t = t_o\text{-}2]$). On onset day ($[t = t_o]$), these positive anomalies intensify and expand, affecting much of the blocking region. In addition, negative (positive) GH anomalies at 500 hPa appear in phase with potential vorticity (PV) anomalies at 200 hPa and relative vorticity (RV) at 850–200 hPa. The positive PV anomalies, at high levels, result from the incursion of PV from mid-latitudes towards the pole. On decay day ($[t = t_d]$), positive anomalies of GH, PV and RV are still found in the blocking region, but with lower amplitude. After the decay day, the anomalous anticyclonic center (positive GH, PV, and RV anomalies) gradually propagates westward (southeastward) in SEP (SAT). Finally, the RV anomalies, in the blocking region, extend from low to high levels of the troposphere, characterizing the barotropic structure for consecutive days.

**Keywords** Blocking episodes · Geopotential · Relative · Potential vorticity

## 1 Introduction

The importance of studying atmospheric blocking relies on the fact that it leads to atypical weather conditions in large scale, in both hemispheres (Treidl et al. 1981). The persistence of atmospheric blocking causes long-lasting heat waves, abnormally dry periods, and stagnant-air conditions (Röthlisberger and Martius 2019). Dry air and precipitation below climatological average associated with the presence of the anomalous anticyclone have a high impact on human activities (Kayano 1999). Atypical weather conditions, precipitation reduction and temperature increase, in both hemispheres, are a consequence of the abrupt interruption of the transient systems, which move around the periphery of the blocking anticyclone (Knox and Hay 1984; Mendes et al. 2005).

Therefore atmospheric blocking has drawn the attention of the meteorological community worldwide (Ruthlant and Fuenzalida 1991; Burkhardt and Lupo 2005; Sinclair 1996; Mendes et al. 2012, Mendes et al. 2014; Rodrigues and Woollings 2017; Mendes et al. 2019; Lupo et al. 2019). Sinclair (1996) and Wiedenmann et al. (2002) when analyzing the frequency of atmospheric blocking observed a smaller

✉ Monica Cristina Damião Mendes
mcdmendes@gmail.com

✉ Maria Regina da Silva Aragão
silva_aragao@yahoo.com.br

[1] Universidade Federal de Campina Grande, Centro de Tecnologia e Recursos Naturais, Unidade Acadêmica de Ciências Atmosféricas, Rua Aprígio Veloso 882, Bairro Universitário, Campina Grande, Paraíba 58.429-900, Brazil

[2] Departamento de Meteorologia, Universidade Federal do Rio Grande do Norte, Natal, Rio Grande do Norte, Brazil

[3] NORCE Norwegian Research Centre, Bjerknes Centre for Climate Research, Bergen, Norway

Published online: 12 August 2022

number of events on the Southern Hemisphere (SH) when compared to the Northern Hemisphere (NH). This occurs in part, as a result of a considerably higher zonal index in the SH (Taljaard 1972), and a smaller persistence of the large positive anomalies associated with the blocking anticyclone (Mo 1983). Moreover, the intense westerly winds in the mid and high troposphere reduces the SH blocking duration (Trenberth and Mo 1985).

In the SH blockings occur preferentially in the South Pacific Ocean (Sinclair 1996; Marques 1996), where the flow is relatively weak (Renwick and Revell 1999; Renwick 2005), which causes a concentration of the blockages at lower latitudes in comparison to the NH blockings (Wright 1974). They are most frequent during austral winter (Berrisford et al. 2007; Mendes et al. 2008; Mendes et al. 2012; Berrisford et al. 2007), when zonal wave 3 becomes more evident and plays a dominant role in the majority of blocking events (Marques 1996; Berbery and Nuñez 1989; Trenberth and Mo 1985).

Usually the definition of blocking events is based on the qualitative criteria proposed by Rex (1950a,b). Nevertheless, these criteria were adapted for a more objective methodology, which has been used in several diagnostic studies of blocking (Lejenas and Okland 1983; Trenberth and Swanson 1983; Lejenas 1984; Tibaldi and Molteni 1990; Tibaldi et al. 1994; Marques and Rao 1999; Mendes et al. 2008). Regarding the formation and maintenance of blocking, it is noticed that they are related to various factors, from interruptions of the zonal flow (Tibaldi and Molteni 1990), temporary change into a meridional flow pattern that favors the formation of strong slow-moving or stationary anticyclones (Treidl et al. 1981), barotropic (Simmons et al. 1983) or baroclinic instability (Frederiksen 1982, 1983), amplification of Rossby waves (Berrisford et al. 2007; Nakamura and Huang 2018), Rossby wave breaking (Pelly and Hoskins 2003), propagation of large-scale waves (Renwick 1998, Renwick and Revell 1999) or, more recently, the contribution of latent heat release (Pfahl et al. 2015). The number of factors and impacts involved in blocking demonstrates the need to further study in detail the behavior of this phenomenon and the characteristics of the atmospheric circulation during each phase of blocking activity.

Previous works showed the decisive contribution of synoptic eddies for blocking formation (Mullen 1987; Shutts 1983; Colucci and Alberta 1996; Nakamura et al. 1997; Drouard and Woollings 2018; Drouard et al. 2021). Thus, synoptic eddy feedback (Berckmans et al. 2013; Shutts 1983) is important for blocking maintenance, and determines their duration, which has a strong impact over the weather. Drouard and Woollings (2018) concluded that blocking events are more influenced by high-and-low-frequency dynamics than by the storm tracks, while Burkhardt and Lupo (2005) verified that blocking events are associated with the planetary-synoptic-scales. In addition, a maximum of Rossby wave activity is observed before blocking formation (Pelly 2001; Pelly and Hoskins 2003; Berrisford et al. 2007). Continuing the studies on atmospheric blocking, some researchers found that interannual variability of blockings is strongly modulated both by ENSO (Marques 1996; Mendes 2007; Renwick 1998; Lupo et al. 2019), and the Antarctic Oscillation phases (Mendes et al. 2012).

In recent years, a growing number of studies use the Potential Vorticity (PV) to detect blockings in both hemispheres (Hoskins et al. 1985; Pelly and Hoskins 2003; Berrisford et al. 2007). Pelly and Hoskings (2003), based on a daily index of the meridional differences of potential temperature, found a reversal of the typical equatorward gradient of potential temperature over the storm track region, and blocking. Once a blocking is established, air parcels are advected from low to high latitudes and vice versa, favoring the reversal of the meridional gradient of potential temperature on a given potential vorticity surface, in such a way that blocking events may be seen as Rossby wave breaking. However, Hitchman and Huesman (2007) emphasized that events on the small scale may also give rise to Rossby wave breaking, both in the troposphere and stratosphere. Therefore, it is possible to assume that not all wave breaks are associated with atmospheric blocking (Berrisford et al. 2007).

While many subjective and objective models have been proposed to explain how atmospheric blocking is formed and maintained (Rex 1950a,b; Lejenas1984; Tibaldi and Molteni 1990; Marques 1996; Pelly and Hoskins 2003; Berrisford et al. 2007), they are unable to depict the life cycle of blocking events, and are concentrated in the Northern Hemisphere. Thus, the present work intends to analyze the average atmospheric patterns, on a large scale, that can be used as indicators of blocking onset and decay in the Southeastern Pacific and South Atlantic, during the period 1979 to 2015 (Fig. 1). These areas are the geographical focus of investigation due to their proximity to the South American continent.

Synoptic-dynamic aspects related to the evolution of blocking events are analyzed through daily analyses of meteorological variables for representative days of the blocking cycle. The datasets used and the processing steps taken are described in the following section. Section 3 discusses the overall climatology of blocking and their seasonal distribution, while Sect. 4 analyzes the atmospheric patterns found before, during and after blocking activity. Discussion and conclusions are given in Sect. 5.

## 2 Data description and identification of blocking events

This study is based on the European Centre for Medium-Range Weather Forecasts (ECMWF) ERA-Interim reanalysis at the 850, 500 and 200 hPa levels, with 2.5 × 2.5 degrees

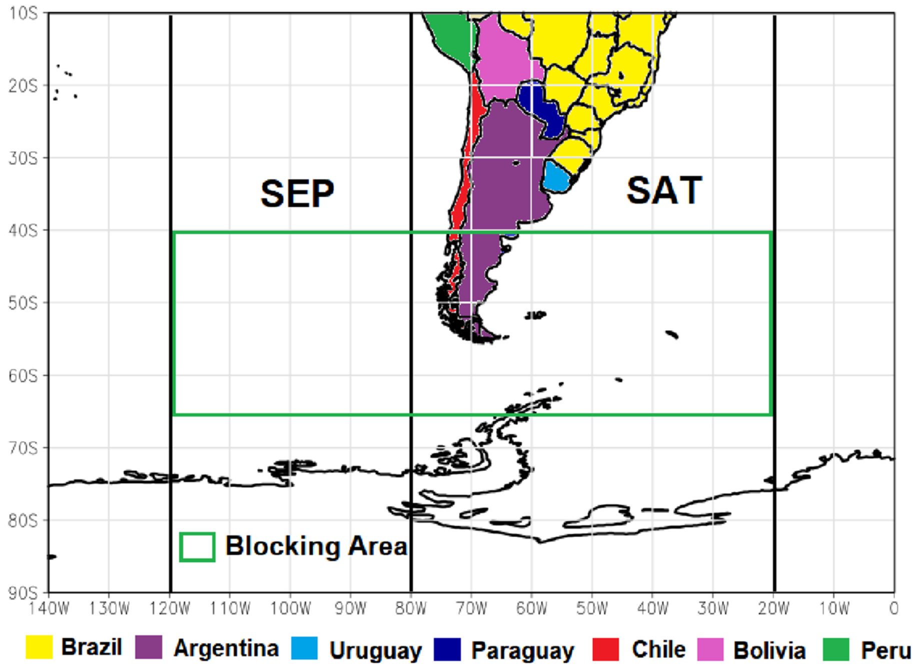


**Fig. 1** Spatial representation of the area of study, subdivided into the sector of the Southeastern Pacific Ocean (SEP), and the sector of the South Atlantic Ocean (SAT). The SEP area comprises the longitudinal band between 120° W and 80° W, and the SAT area is between 80° W and 20° W. The countries are indicated by colors: Argentina (violet), Bolivia (pink), Brazil (yellow), Chile (red), Paraguay (dark blue), Peru (green) and Uruguay (light blue)

latitude–longitude spatial resolution (Dee et al. 2011). This resolution is satisfactory, as we intend to analyze blocking events and associated atmospheric patterns on a large scale. Blocking events are identified in the latitudinal band of 40° S–65° S, within two longitudinal sectors: 120° W–80° W, in the Southeastern Pacific Ocean (SEP), and 80° W–20° W, in the Southern Atlantic Ocean (SAT) (Fig. 1). It is important to note that the study areas meet the criteria proposed and established by Rex (1950a, b).

Geopotential Height (GH); Relative Vorticity (RV); Potential Vorticity (PV); Zonal and Meridional Wind components are used for the analysis of synoptic and dynamic patterns before, during and after the blocking activity, in the two study areas. The atmospheric patterns during blocking events are identified using daily GH data at 500 hPa for the austral summer (December, January, February—DJF) and austral winter (June, July, August—JJA) seasons in the Southern Hemisphere, for the period from 1979 to 2015. These two seasons were chosen because they represent the one with the lowest and highest blocking activity, respectively, in both study areas (see Sect. 3). Furthermore, Sect. 3 presents the climatology for all seasons.

The atmospheric patterns associated with blocking events identified in the 37 years of study are diagnosed for representative days of the blocking cycle. This process considers the following representative days of a blocking event: [($t = t_{o)}$], the onset day; [($t = t_o$-2)], two days before onset; [($t = t_{d)}$] the decay day; and [($t = t_d + 2$)], two days after decay. Onset day is identified as the first day in which the objective criteria of blocking are satisfied (onset of blocking). In contrast, the decay day corresponds to the day in which the blocking index is no longer observed or, in other words, the decay day is defined as the first day in which there is no blocking. Particular attention was given to two days before onset, since this period shows greatest variability concerning the blocking formation. Two days after decay are analyzed also.

The modified Tibaldi index (Tibaldi et al. 1994), applied in Mendes et al. (2008), is used to identify blocking and to obtain its climatology for the period of study. Blocking identification is based on two meridional geopotential height gradients at 500 hPa, defined as Geopotential Height Gradient South (GHGS) and North (GHGN), calculated for both areas, SEP and SAT. The 500 hPa geopotential height meridional gradients GHGS (south) and GHGN (north) are obtained according to Eqs. (1–2) below:

$$GHGS = Z(\lambda, \phi_S) - Z(\lambda, \phi_{02}) \tag{1}$$

$$GHGN = Z(\lambda, \phi_{01}) - Z(\lambda, \phi_N) \tag{2}$$

$\phi_N = 40°S + \Delta$
$\phi_{01} = 55°S + \Delta$
$\phi_{02} = 50°S + \Delta$
$\phi_S = 65°S + \Delta$
$\Delta = -10.0°; -7.5°; -5.0°; -2.5°; 0°$

The Z $(\lambda,\phi)$ is the 500 hPa geopotential height at longitude $\lambda$ and latitude $\phi$; "Δ" represents one latitudinal interval. Then, following the procedure developed by Tibaldi et al. (1994), a given longitude is defined as "blocked" at a specific instant in time if the following conditions are satisfied, for at least one value of Δ: (a) GHGN > 0 and (b)

GHGS < -10 m. A sector is considered blocked on a particular day if three or more adjacent longitudes, within the study area, are blocked (Trigo et al. 2004).

This criterion is sufficient to define a local (spatial) blocking pattern. However, the definition of a true synoptic blocking requires the specification of a certain persistence time for the event, whose typical duration varies between 5 and 30 blocking days (Treidl et al. 1981; Tibaldi and Molteni 1990). The concept of blocking day (Tibaldi et al. 1994; Renwick 2005; Trigo et al. 2004; Wiedenmann et al. 2002; Mendes et al. 2005) refers to a "day" in which the blocking index is observed, while each blocking episode corresponds to a set of blocking days, which has a minimum of five consecutive days.

Composites of anomalous variables were analyzed for each of the four characteristic days previously defined, in order to diagnose the blocking temporal evolution in both sectors, SEP and SAT. The anomalies were obtained taking into account the daily climatology of each variable (for the 37 years, 1979 to 2015). The significance of the composites was tested with the Student's t test at the 90% confidence level, which is applied to examine the significant differences between the climatological patterns and the daily observed patterns related to blocking. With this approach the aim is to identify large coherent areas (particularly over the continents) that experienced unusual conditions due to blocking episodes. The statistical test (*Student's t test*) applied here has the null hypothesis of equal average, unilateral, with t critical that depends on the quantity of blocking episodes found in each sector, and in each season of the year. This test was also used by Hansen et al. (1982, 1983) in composite analysis. Finally, the composite (Figs. 3, 4, 5, 6, 7, 8, 9, 10) shows the synoptic-dynamic patterns associated with blocking events in SAT and SEP, for summer (DJF) and winter (JJA).

## 3 Blocking climatology

The frequency and general distribution of blocking events for each month, season and sector is shown in Fig. 2. The maximum number of blocking events and blocked days, in both sectors, occur between the months of May and August (Fig. 2a, b). The transition months (autumn and spring) show no significant difference between the number of blocking days and events. It is worth noting that the events and blocking days are higher in the month of May in SAT, while they are predominant in June over SEP (Fig. 2). Furthermore, the frequency of events and blocking days in SEP are practically twice of SAT. These results are in agreement with other authors that have used either similar (Marques and Rao 1999, 2000) or different blocking methodology (Renwick and Revell 1999).

In winter and spring (Table 1), the blocking events in SEP (SAT) have a mean duration between 7.00 and 9.03 days (7.02 and 7.26 days). Furthermore, in autumn, the blocking events lasting longer than five days are more numerous in SEP. The higher frequency of blocking episodes from June to September is to be associated with the more intense meridional thermal gradient observed at this time of the year, and to the northward displacement of the Polar and Subtropical jets (Mendes et al. 2008).

Additionally, in summer and autumn (Table 1), the blocking events which occur in SEP (SAT) have a mean duration between 6.75 and 8.20 days (5.92 and 8.00 days). In summer months, when blocking frequency declines over the Southeastern Pacific, the subtropical jet practically vanishes over South America, and the polar jet prevails at higher latitudes (Pezzi and Cavalcanti 1994). Note also that most blocking events have duration between 5 and 10 days, and only 2.7% last longer than 16 days. The most

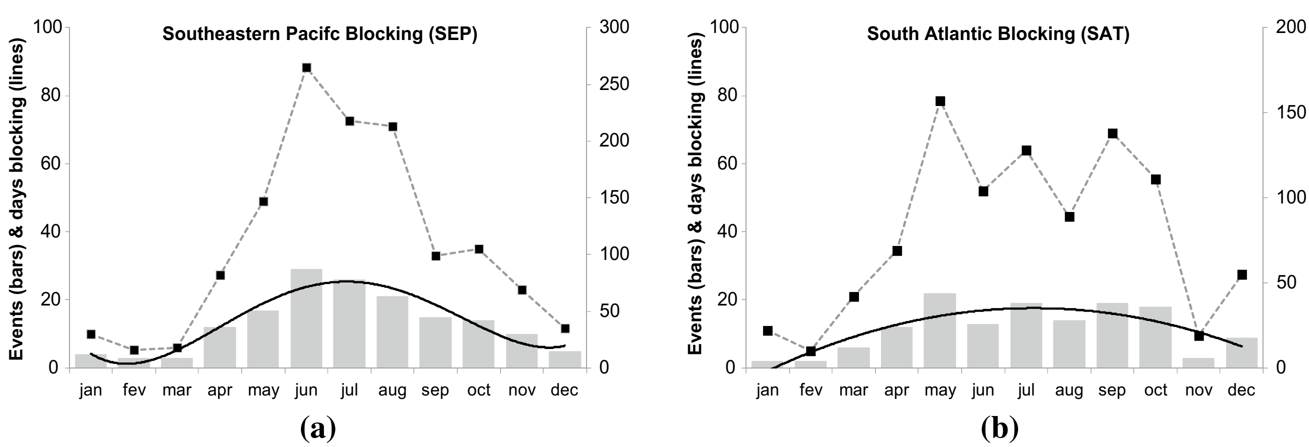


**Fig. 2** Monthly distribution of the total number of blocking events (columns) and blocked days (lines) for (**a**) Southeastern Pacific and (**b**) South Atlantic in the period 1979–2000

**Table 1** Total number of blocking events, total number of blocking days, mean duration, maximum duration, classes of blocking duration in the Southeastern Pacific (SEP) and South Atlantic (SAT)

| SEASONS | Winter | | Spring | | Autumn | | Summer | |
|---|---|---|---|---|---|---|---|---|
| Areas | SEP | SAT | SEP | SAT | SEP | SAT | SEP | SAT |
| Duration (days) | Events | | Events | | Events | | Events | |
| 5–10 | 57 | 41 | 33 | 33 | 23 | 35 | 11 | 13 |
| 11–15 | 15 | 2 | 6 | 5 | 8 | 5 | 1 | – |
| 16–20 | 3 | 2 | – | – | 1 | – | – | – |
| 21–25 | 2 | – | – | – | – | – | – | – |
| ***Mean duration** (days)* | 9.03 | 7.26 | 7.00 | 7.02 | 8.20 | 8.00 | 6.75 | 5.92 |
| Areas | SEP | SAT | SEP | SAT | SEP | SAT | SEP | SAT |
| ***Total of Blocking Days*** | 696 | 330 | 273 | 274 | 247 | 268 | 81 | 77 |
| ***Total** of **Events*** | 77 | 45 | 39 | 38 | 32 | 40 | 12 | 12 |
| ***Maximum duration** (days)* | 25 | 19 | 14 | 16 | 20 | 13 | 12 | 9 |

long-lasting blocking in SEP was identified in 1986, with 25 days of activity (July 24th to August 16th).

This result was also found by Marques (1996) using a distinct methodology for identification of blocking as well as a different database (NCEP/NCAR reanalysis). Marques, obtained a total of 17 blocking days for this event in SEP and draws attention to the importance of the subtropical and polar jets, and of large-scale tropical disturbances for its formation and maintenance. In SAT, the longest-lasting blocking event occurred in 1984, from August 8th to 26th, with 19 days of activity (Table 1).

The annual frequency of blocking events (FBe) for the years EN (El Niño), LN (La Niña) and N (Neutral) is presented in Table 2. The total years with EN (El Niño), LN (La Niña) and N (Neutral) is calculated by adding the number of years classified as EN (LN, N), and dividing the result by the total of years (37 years, 1979–2015). Finally, the result is multiplied by 100. The monthly distribution of the total number of blocking events (columns) and blocked days (lines) is shown in Fig. 2. The SEP sector presents a rate of 4.3 events per year, which are evenly distributed throughout the years. However, when comparing to their NH counterparts it is observed a smaller number as found by other authors (Sinclair 1996; Wiedenmann et al. 2002).

The South Atlantic sector shows about 3.3 events per year, which are evenly distributed throughout the period. These results are consistent with those found by Burkhardt and Lupo (2005), who concluded that the events have smaller duration and are less intense in the SH as compared to the NH. The interannual distribution of the number of events shows high variability for both SAT and SEP sectors (Table 2). In both sectors, more events and blocking days were found in EN years. These results are consistent with those obtained by Mendes (2007) and Wiedenmann et al. (2002), and are in disagreement with those found by Marques (1996). In SEP, the frequency of events in EN years varies between 62 and 66%, i. e, more than half of the years with blocks occur with SST above the climatological average. In SAT, blocking events have a higher frequency in EN (LN) years, in transition (summer and winter) months.

## 4 Atmospheric patterns associated with South Atlantic (SAT) blocking events

The life-cycle of atmospheric blocking has been a widely discussed topic in the literature, both from a dynamical point of view, and of the synoptic-scale perturbations. The composites presented in this section document the activity of blocking in SAT sector, in austral summer (DJF) and austral winter (JJA). Figures 3, 4, 5, 6 show the anomalous patterns of potential vorticity (PV) at 200 hPa;

**Table 2** Total number of blocking events in EN (El Niño), LN (La Niña) and Neutral years as a percentage, and total number of events per years for the Southeastern Pacific (SEP) and South Atlantic (SAT) sectors

| Seasons | Winter | | Spring | | Autumn | | Summer | |
|---|---|---|---|---|---|---|---|---|
| Areas | SEP | SAT | SEP | SAT | SEP | SAT | SEP | SAT |
| Neutral years (percentage) | 6.49 | 6.7 | 15.4 | 13.2 | 9.3 | 20 | 16.6 | 0 |
| EN years (percentage) | 62.3 | 44.5 | 66.7 | 48.7 | 65.5 | 45 | 66.8 | 41.7 |
| LN years (percentage) | 32.2 | 48.8 | 17.9 | 39.4 | 28.2 | 35 | 16.6 | 58.3 |
| **Total (per years)** | 2.08 | 1.21 | 1.06 | 1.03 | 0.87 | 1.08 | 0.33 | 0.32 |

geopotential height (GH) at 500 hPa; relative vorticity (RV) at 200 and 850 hPa and wind anomalies at 200 and 850 hPa.

Examining the PV, it is important to keep in mind that upper-tropospheric and stratospheric PV patterns are associated with many atmospheric flow phenomena. A characteristic of blocking formation can be viewed as positive upper-level PV anomalies that are linked to surface weather patterns (Sprenger et al. 2007), which are associated to a large-scale extended ridge; within a Rossby wave pattern (Woollings et al. 2018). Additionally, PV is frequently considered in dynamics investigation of blocking (Bluestein 1993; Pelly and Hoskins 2003; Schwierz et al. 2004; Iwabe 2008). However, the ridge extension of the PV occurs within 3 days, associated with both planetary-scale waves and baroclinic waves in synoptic-scale weather systems (Woollings et al. 2018).

Upper–level PV positive perturbations can induce upward/downward air motion in the middle and lower troposphere downstream/upstream of the perturbations (Hoskins et al. 1985, 2003), and are associated with tropospheric air intrusion in middle and high latitudes. Meanwhile the negative PV anomalies are associated with the intrusion of stratospheric air. Positive PV anomalies at high levels, two days before onset ([t = $t_o$-2]), seems to be an indicator of blocking formation in both seasons (Fig. 3a, b). In fact, PV increase, within the blocking region, interrupts the predominance of negative PV anomalies, found in a large part of the SH. Moreover, in summer, negative PV anomalies are identified in the south of South America (Fig. 3a). In

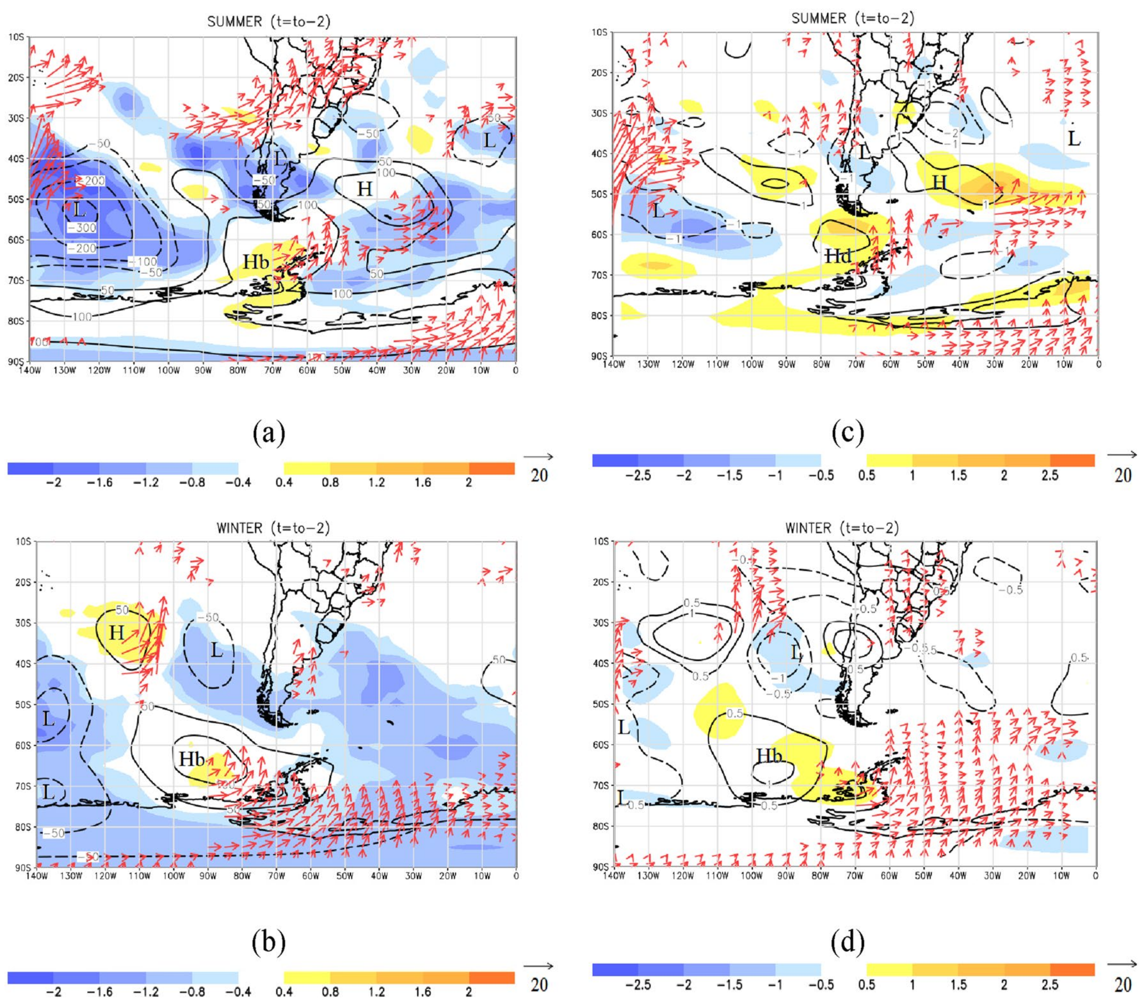


**Fig. 3** Composites of SAT blocking for two days before onset [(t = $t_o$-2)]: (**a**, **b**) Potential Vorticity Anomalies (colors, $*10^{-6}$ K kg$^{-1}$ m$^2$s$^{-1}$) and Wind Anomalies at 200 hPa (red vectors, ms$^{-1}$), Geopotential Height Anomalies at 500 hPa (contours, mgp); (**c**, **d**) Relative Vorticity Anomalies ($*10^{-5}$ s$^{-1}$) at 200 hPa (colors) and 850 hPa (contours), Wind Anomalies at 850 hPa (red vectors, ms$^{-1}$). The blocking events and days are obtained using ERA-Interim data (1979–2015) for austral (**a**, **c**) summer (DJF) and (**b**, **d**) winter (JJA). The wind scale (ms$^{-1}$) is seen to the right of the color scale. The location area of the blocking anticyclone is indicated by Hb. A t-test at the 90% confidence level was applied

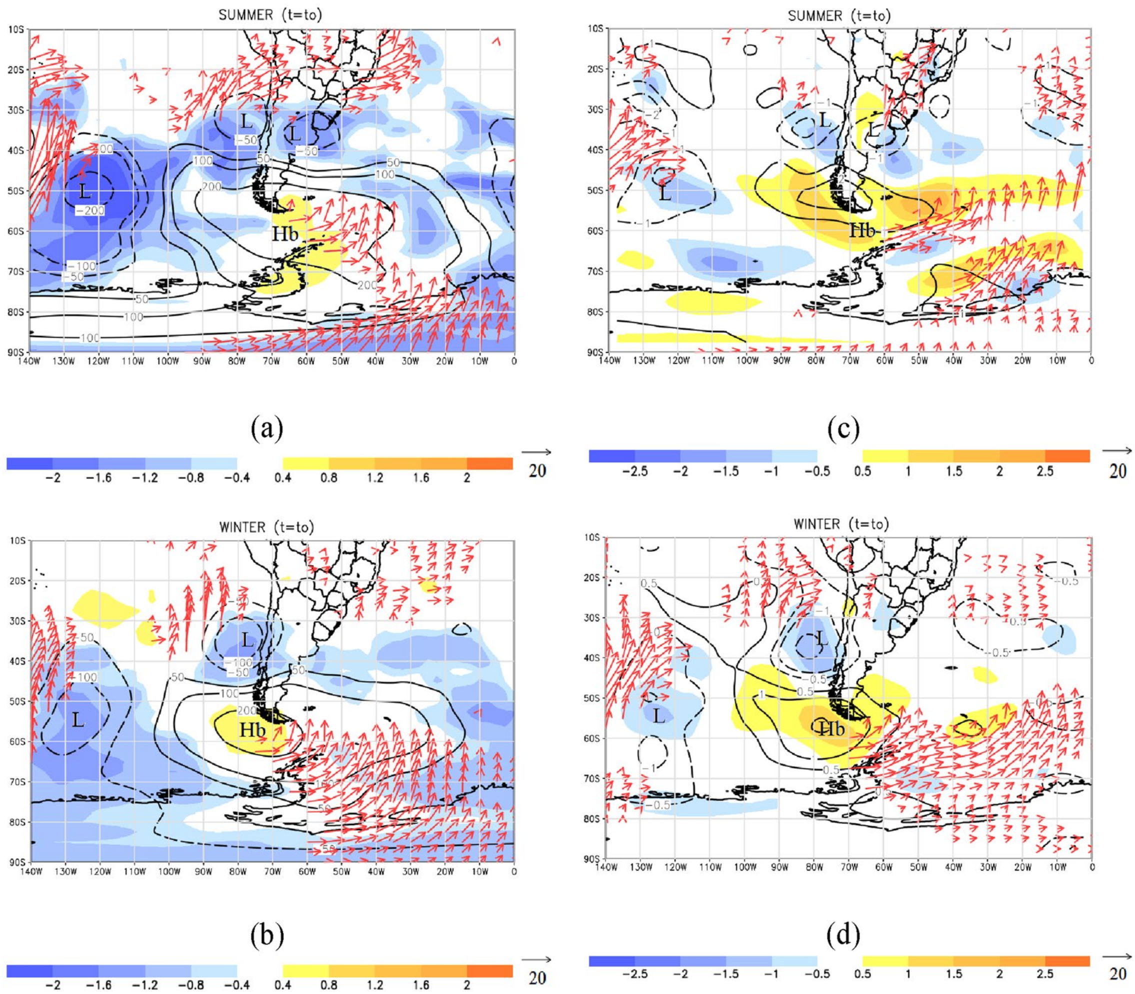


**Fig. 4** As in Fig. 3 but with respect to composites for onset day [(t = $t_o$)]

winter, another center de positive PV anomaly is found in mid-latitudes (Fig. 3b).

Patterns similar to those found here were observed by Mendes et al. (2019), whom observed distortions in the tropopause, characterized by tongues of anomalously high PV, extending towards the equator, during atmospheric blocking action. It is worth noting that the positive PV anomalies accompany the blocking anticyclone, and are relatively smaller in winter (Fig. 3b), compared to those found in summer (Fig. 3a). Another important aspect is that the positive (negative) PV anomalies at high levels are in phase with positive (negative) GH anomalies at mid-levels. This process favors the presence of positive GH anomalies, stretched in a northwest–southeast (northeast–southwest) configuration, two days before onset ([t = $t_o$-2]) in SAT (Fig. 3a, b).

Thus, the configuration of PV anomalies at 200 hPa seems to modulate, in part, the geopotential height field at 500 hPa into a distinctive shaped pattern of Omega-type (Ω) blocking studied by Marques and Rao (1999) and others. In both seasons, the anomalous anticyclone shows up meridionally aligned with a low located on its northern flank, while an extensive and stronger low is seen to the west. Due to its horizontal dimensions, Omega blocking tends to be quite persistent and cause flooding on the north-northeast flank of the anticyclone (Mendes et al. 2005).

Furthermore, cyclonic centers (negative GH anomalies) located to the west of the blocking high, in mid-latitudes of the South Pacific, two days before onset ([(t = $t_o$-2)]) are accompanied by significant anomalous winds upstream (Fig. 3a-d). This pattern is a result of the frequency of transient systems that are displaced on the periphery of the blocking anticyclone. This result corroborates those obtained by Berbery and Núnez (1989) and Mendes et al. (2005, 2008)).

Traditionally, the significant anomalous winds tend to have higher magnitudes on the eastern flank and or downstream of the blocking anticyclone (isentropic PV gradient and positive GH anomalies). This last one favors

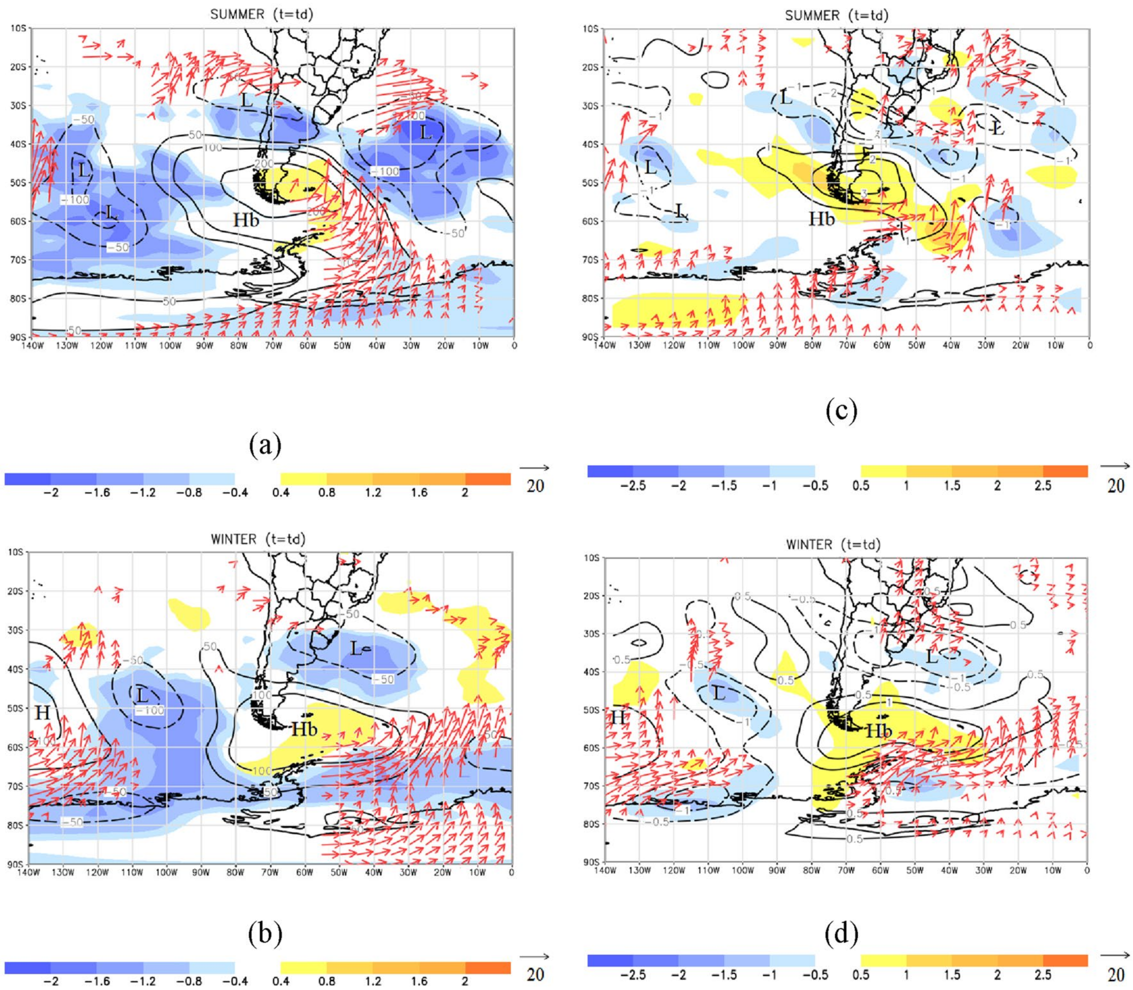


**Fig. 5** As in Fig. 3 but with respect to composites for decay day [($t=t_d$)]

the splitting of the jet into two branches, one in the subtropics, the subtropical jet (STJ), and the other one in mid-latitudes, the sub-polar jet (SPJ). In summer, the subtropical branch is indicated by the significant anomalous west-southwesterly winds that accompany the low (negative GH anomalies) located to the north of the blocking anticyclone. Furthermore, anomalous winds are seen over the continent two days before onset [($t=t_o$-2)] (Fig. 3a, b).

Finally, in summer, centers of positive RV anomalies (Fig. 3c) are found two days before onset [($t=t_o$-2)], being in phase with the positive PV anomalies (Fig. 3a). It is highlighted that the negative (positive) RV anomalies, correspond to anomalous cyclonic (anticyclonic) circulation in the Southern Hemisphere (SH). Also, two days before onset ([$t=t_o$-2]) anticyclonic RV associated with the blocking high is located to the south of South America (Fig. 3c, d). Anticyclonic RV (positive RV anomalies) seen in the area of the blocking anticyclone, has the same sign along the vertical, from high to low levels, indicating an equivalent barotropic condition of the blocking (Takaya and Nakamura 2005).

Figure 4 shows the composites for onset day in summer (a, b) and winter (c, d) over SAT. Observations have frequently shown that blocking formation involves the interaction between planetary-scale waves, Rossby waves of different wavelengths and local-scale waves (Austin 1980; Marques and Rao 1999; Luo 2005). On onset day ([$t=t_o$]), positive PV anomalies are more pronounced (Fig. 4a, b), with larger longitudinal/latitudinal extension, compared to two days before (Fig. 3a, b). This result is in line with those obtained by Hoskins et al. (1985) and Shutts (1983), who analyzed the presence of an injection of equatorial low magnitude PV air, during blocking activity.

In both seasons, the positive PV anomalies are northeastward displaced, being located on the tip of the South American continent (Fig. 4a, b). The relatively strong PV gradient between the blocking region and the north flank is clearly visible during onset day ([$t=t_o$]). Thus, meridional

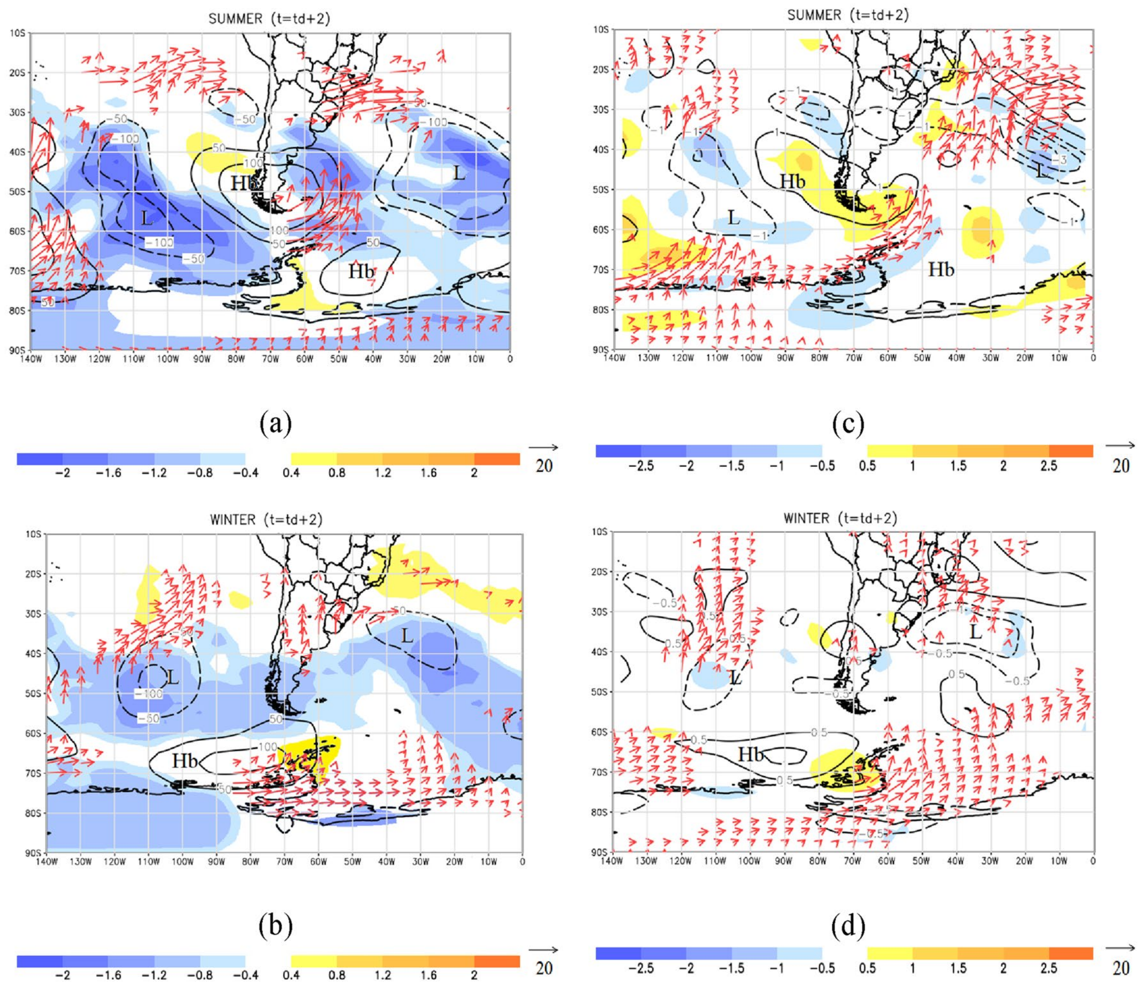


**Fig. 6** As in Fig. 3 but with respect to composites for two days after decay [(t = $t_{d+2}$)]

PV gradient is reversed with anticyclonic PV anomaly (positive values) on the poleward side and cyclonic anomaly (negative values) on the equatorial side. This situation is often described and also pictured in Burkhardt and Lupo (2005).

Regarding, the positive GH anomalies on onset day ([t = $t_o$]), it can be seen that they are better configured, occupying considerably larger areas, with values equal to or greater than 100 mgp (Fig. 4a, b). In summer, the positive center has a northwest-southeast configuration (Fig. 4a), while in winter it shows a zonal configuration (Fig. 4b). In both seasons, the positive center of GH anomalies is slightly displaced north-eastward compared to two days before onset (Fig. 3a, b), remaining in phase with the positive PV anomalies.

On onset day [(t = $t_o$)] the positive PV centers (Fig. 4a, b), are more evident than two days before (Fig. 3a, b). Moreover, the semi-stationary blocking in summer (winter) causes changes in the usual trajectory of synoptic systems (*e.g.*: extratropical cyclones, frontal systems, storm-tracks), favoring negative GH anomalies and negative PV anomalies in central Chile, central Argentina and Uruguay (central Chile and west Argentina) (Fig. 4a, b). Anomalous winds are seen over the continent in the South Atlantic Ocean (Figs. 3 and 4). Analogously to Fig. 3c-d, the configuration of the RV anomalies indicates the barotropic equivalent condition of the blocking, in which positive RV anomalies extend from high to low tropospheric levels over the blocking region. Additionally, a center of positive RV anomalies has higher magnitude and larger area (Fig. 4c) in comparison with two days before.

On decay day ([t = $t_d$]), areas with positive PV anomalies found in the blocking region are slightly displaced north-eastward (eastward) in summer (winter) (Fig. 5a, b). This eastward displacement tends to weaken the blocking itself, by inducing a zonal narrowing of PV anomaly areas, while maintaining their spatial scale. This is in agreement with the previous work of Nakamura et al. (1997), whom already noted an eastward shift of the low-PV center, concurrent with the slow retrogression of the high pressure center once blocking decay begins. This influences the transient systems in ways that preferentially intensify the low PV anomaly, and also acts to maintain the block (Luo et al. 2014). It should be noted also, that areas of negative PV anomalies increased and intensified downstream of the blocking anticyclone over time (Fig. 5a, b). Meanwhile, negative PV anomalies located in south Brazil, Uruguay and Argentina are weaker and eastward displaced.

Moreover, on decay day ([t = td]), the center of positive GH anomalies associated with the blocking anticyclone has smaller area, in both seasons (Fig. 5a, b). Concerning the magnitude, positive GH anomalies are unchanged in summer (Fig. 5a), and weaker in winter (Fig. 5b). In turn, negative GH anomalies are found in summer (winter) over central Chile and central-western Argentina (extreme southern Brazil, Uruguay, northeastern Argentina and eastward extension over the subtropical South Atlantic) (Fig. 5a, b). An extensive and strong center is also seen over the subtropical South Atlantic, in summer (Fig. 5a). In addition, positive (negative) mid-tropospheric GH anomalies remain in phase with positive (negative) upper tropospheric PV anomalies, in both seasons (Fig. 5a, b). Finally, significant winds are again seen over Brazil (Fig. 5b–d).

Note, however, that the positive RV centers increase in area up to the decay day ([$t = t_d$]) (Fig. 5c, d), while propagating north-eastward, influencing the tip of the South American continent. In turn, negative RV anomalies located on the northern flank of the blocking anticyclone intensify and extend zonally (Fig. 5c, d). In winter, positive RV anomalies at high and low levels shift slightly eastward (Fig. 5d), while in summer there are no significant changes (Fig. 5c). Cyclonic circulation (negative RV anomalies) is found downstream from the Andes on decay day ([$t = t_d$]) and, in general, is associated with storm tracks (Mendes et al. 2007). Therefore, the negative RV anomalies play an important role in the formation and maintenance of the blocking itself (Colucci 1985). In contrast, anticyclonic circulation (positive RV anomalies) is seen on the bottom left-hand corner of the map.

Two days after decay ([$t = t_d + 2$]), in summer, the blocking high (positive GH anomalies), centered on the tip of the South American continent, has its area and magnitude considerably reduced, while the positive PV center is displaced north-westward (Fig. 6a). Negative PV anomalies dominate central-eastern Argentina, and the eastern flank of the blocking anticyclone, while negative PV and GH centers are in phase downstream (Fig. 6a). In winter, the blocking high and its associated positive PV anomalies are south-westward displaced and considerably reduced longitudinally, but with unchanged magnitude (Fig. 6b). The negative GH and PV anomalous centers remain in phase and are slightly displaced east-southeastward over the subtropical South Atlantic. Positive PV anomalies are identified over southeastern Brazil. This particular pattern favors the southeastward shift of the band of negative PV anomalies, located in Chile, Argentina and south Brazil.

The area occupied by the positive RV centers on two days after decay ([$t = t_d + 2$]) is considerably reduced and displaced south-westward, with the equivalent barotropic structure hardly seen (Fig. 6c, d). However, while the significant anomalous southerly winds, associated with the blocking anticyclone, weaken, the west-southwesterly wind located on the storm track area extends in southern South America (Fig. 6a–d). This result corroborates with that found by Adana and Colucci (2005), whom suggest that the increase in anticyclonic flow, forced by the geostrophic relative vorticity, near the blocking region, contributes also for block formation in some cases. Finally, positive (negative) RV anomalies (Fig. 6c, d) remain in phase with positive (negative) GH anomalies at 500 hPa (Fig. 6a, b). This process maintains the barotropic condition of the block which, along with the feedback of transient eddies, are important for maintaining the remnant of atmospheric blocking.

## 5 Atmospheric patterns associated with Southeastern Pacific (SEP) blocking events

Long-lasting blockings are frequently observed over the Southeast Pacific (SEP), and are favored by the presence of the Subtropical and Polar jets and transient disturbances (Mendes et al. 2005). Another contribution to the formation and maintenance of blockings in this sector is the amplification of waves 1 and 3 (Marques 1996). In analogy with the previous section, the focus here is the blocking activity in SEP, in austral summer (DJF) and winter (JJA). Figure 7a-d shows composites of GH anomalies at 500 hPa; PV anomalies at 200 hPa; RV anomalies at 850–200 hPa and wind anomalies at 200 and 850 hPa, for two days before onset [($t = t_o$-2)].

A positive GH anomaly center (blocking high) is observed in the Southeast Pacific, two days before onset [($t = t_o$-2)] (Fig. 7a, b). It is worth noting that blocking appears as a center of positive PV anomalies within a large area of negative values. Clearly, the positive PV anomalies indicate that tropospheric air from low latitudes is being entrained into higher latitudes, as observed by Hoskins et al. (1985) and Shutts (1983) for blockings in the Northern Hemisphere. It is still possible to note the presence of negative PV anomalies in southern Chile and Argentina when blocking is established in SEP. Again, note that the positive (negative) PV anomalies, similarly to that observed on the SAT, are in phase with positive (negative) GH anomalies.

Regarding the significant anomalous winds, the position of the blocking high (anticyclonic circulation) seems to favor intense south-southwesterly wind anomalies on its eastern

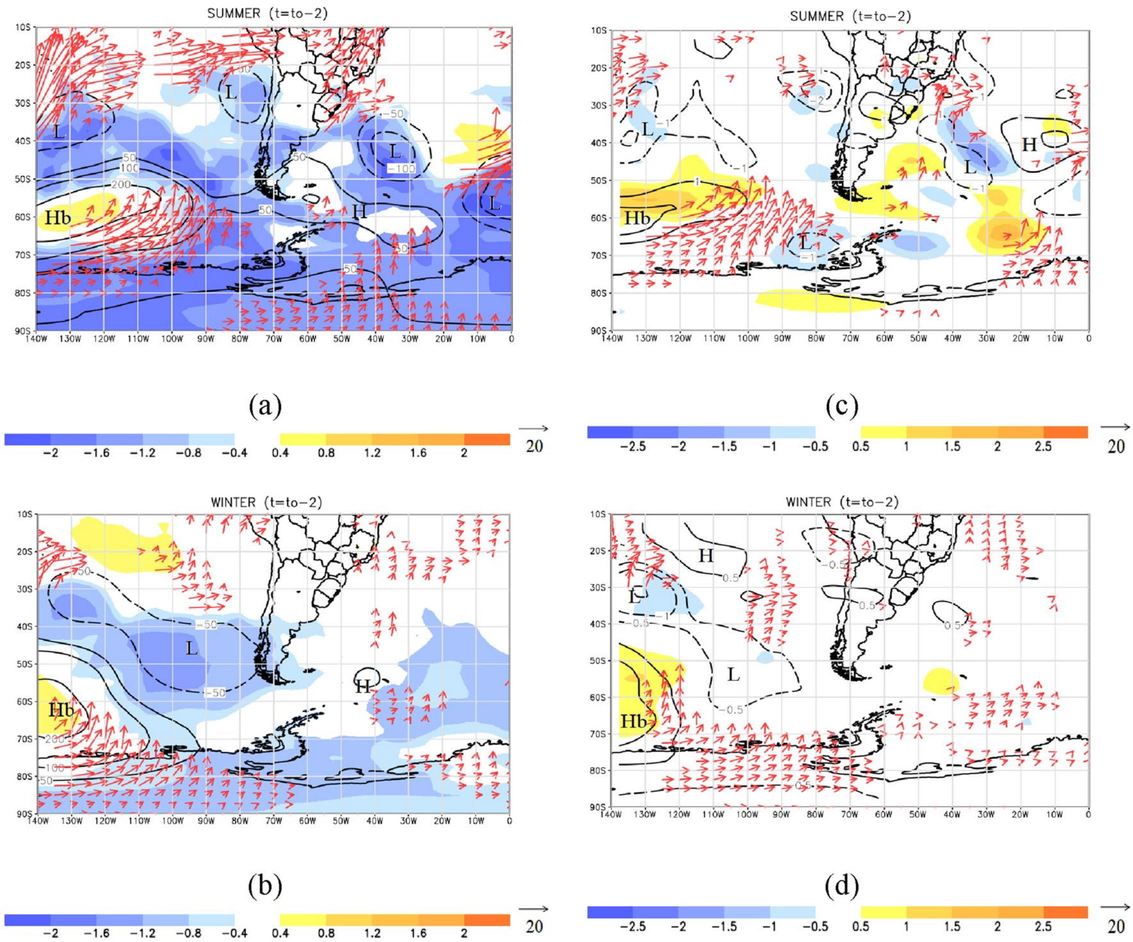


**Fig. 7** As in Fig. 3 but with respect to composites in the Southeastern Pacific

flank and downstream, in both seasons (Fig. 7a, b). In summer, west-southwesterly winds are seen over Peru, Brazil and nearby oceanic areas (Fig. 7a). In turn, the composites of RV anomalies at 850–200 hPa (Fig. 7c, d) show that the positive (negative) centers are in phase with the positive (negative) GH centers in the middle troposphere, and also with the PV centers in the high troposphere (Fig. 7a, b). The barotropic condition can be confirmed by the presence of a semi-stationary high (anticyclonic circulation), which extends from 200 to 850 hPa. Overall, the temporal evolution of the patterns in Fig. 7a–d resembles those in Fig. 5a–d, in magnitude and extension.

Nevertheless, the anomalous wind patterns, in summer months, are quite different in the upper troposphere, as compared to the lower troposphere. Again, the barotropic structure of the blocking is found in the form of a center of positive RV anomalies that extends along the troposphere, in the blocking region (Fig. 7c, d). The barotropic structure of the blocking seems to be associated with transient eddy forcing which, in turn, favors blocking development (Karoly 1983; Takaya and Nakamura 2005).

Similarly to that found for SAT, on onset day ([$t=t_o$]), the positive GH and PV anomalies become more pronounced (Fig. 8a, b), with increased longitudinal/latitudinal extension, compared to two days before [($t=t_o$-2)] (Fig. 7a, b). The magnitude of the blocking high reaches 400 gpm, the highest one throughout the life cycle. The center of positive PV anomalies is surrounded by areas of negative anomalies, which extend over large areas of both oceans. Such results are coherent to some degree with those exposed by Hoskins et al. (1985). Hoskins et al. (1985), analyzing the time evolution of blocking events over the NH, concluded that injection of equatorial PV air into the blocking areas, is followed by the passage of deflected transient synoptic weather systems.

Moreover, negative PV anomalies are observed over central-southern (southern) Chile and Argentina, in summer (winter) (Fig. 8a, b). In turn, the pattern of negative GH anomalies located to the north of the positive GH anomalies indicates the prevalence of dipole-type blocking over SEP. The positive RV areas are strengthened, covering a larger longitudinal extension, and are flanked by smaller centers with negative RV anomalies (Fig. 8c, d). In addition, the

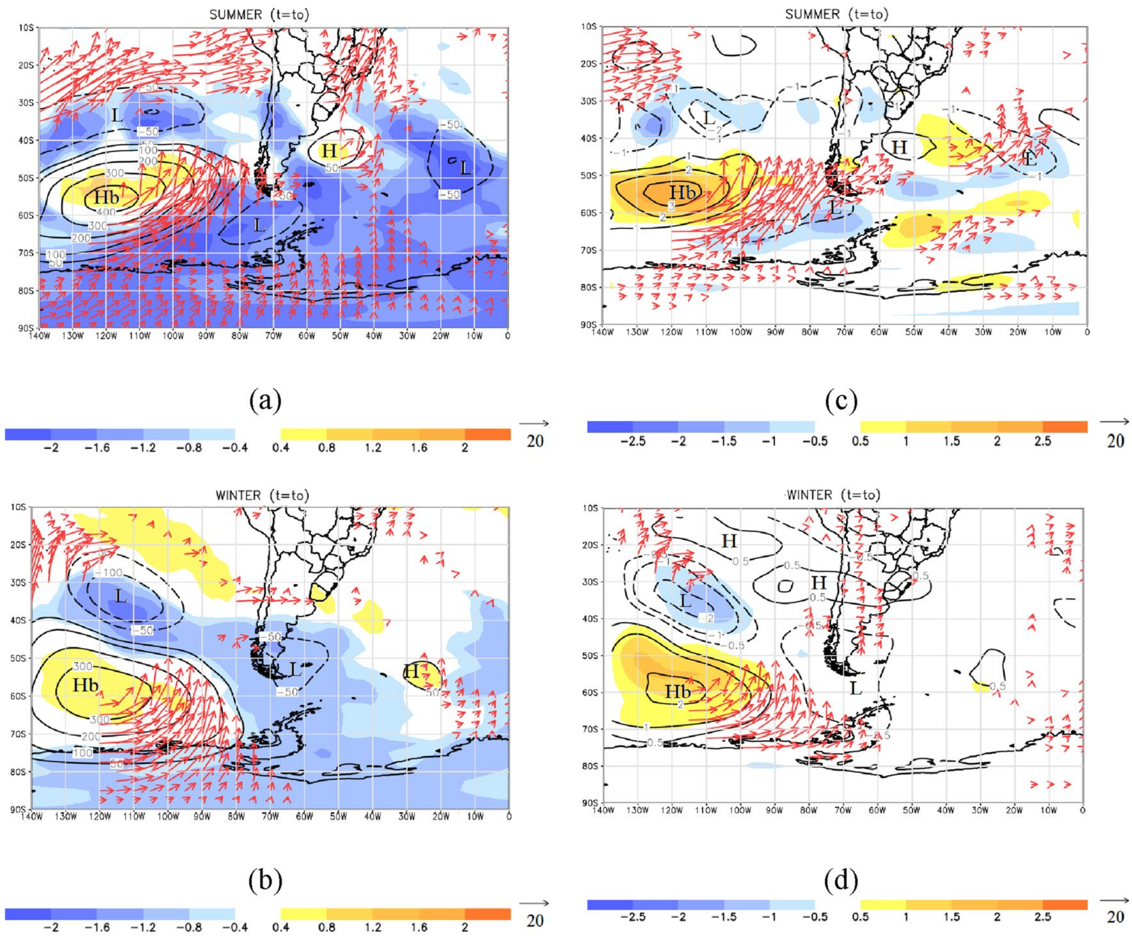


**Fig. 8** As in Fig. 4 but with respect to composites in the Southeastern Pacific

position of the blocking anticyclone (anticyclonic circulation) seems to favor intense southerly winds downstream (Fig. 8a–d). In this way, the blocking anticyclone amplifies the climatological meridional flow both upstream and downstream, keeping itself active. Finally, the centers of positive GH anomalies at 500 hPa, also appear in phase with the centers of positive PV anomalies, as found in SAT.

On decay day ($[t=t_d]$), positive PV and GH anomalies are still in phase in the blocking region, but eastward displaced, particularly in winter (Fig. 9a, b). Areas of negative PV anomalies are better defined around the blocking region, being coupled with larger and stronger centers of negative GH anomalies, eastward of the blocking region (Fig. 9a, b). Negative GH anomalies are also found in the south of South America. Positive RV anomalies are weaker and cover smaller areas, while centers of negative RV anomalies are strengthened, and cover a significant area northward and eastward of the blocking anticyclone (Fig. 9c, d). Anomalies found in the equatorial flank, that extend zonally favors the trajectory of the transient systems in the extreme south of South America (storm tracks). Finally, wind and PV anomalies are also seen over parts of South America and the South Atlantic, particularly on decay day ($[t=t_d]$) (Fig. 9a-d).

Two days after decay ($[t=t_d+2]$), in summer, the blocking anticyclone and its associated positive PV anomalies are weaker and westward displaced (Fig. 10a). Additionally, the negative centers keep their magnitude and are displaced eastward. In winter, the positive PV centers are displaced southeastward, while the blocking anticyclone becomes weaker (Fig. 10b). The positive PV anomalies, in summer (winter), occur over Uruguay and central-eastern Argentina (over Patagonia) (Fig. 10a, b). In summer, over South America, negative PV anomalies are found southward of 40°S. In winter, negative PV anomalies cover part of the area southward of 30°S, approximately. The positive RV anomalies centers, in the blocking region, remain extending throughout the troposphere, but are less intense, while negative RV anomalies predominate, in summer (Fig. 10c, d). Also, strong west-southwesterly winds indicate a northward displaced subtropical jet, while over the

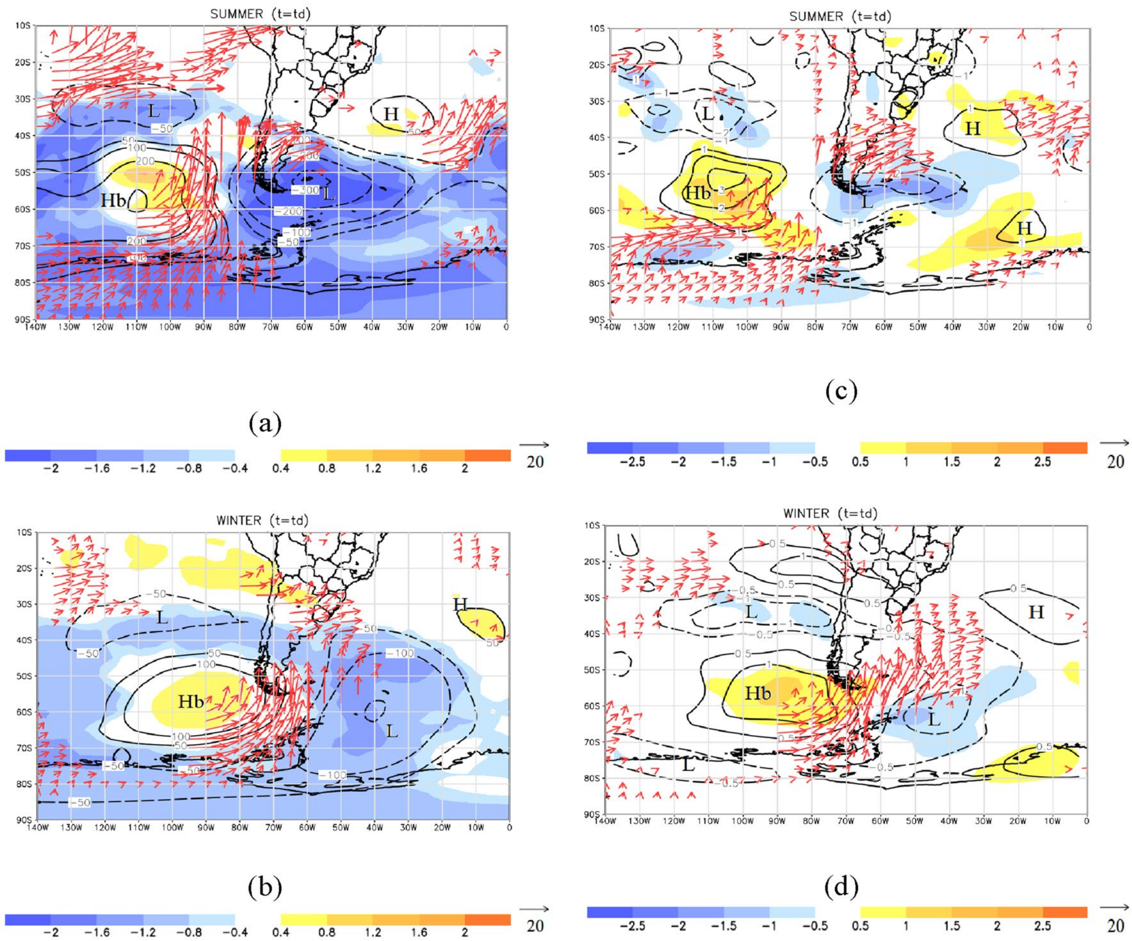


**Fig. 9** As in Fig. 5 but with respect to composites in the Southeastern Pacific

South Atlantic anomalous winds are associated with anticyclonic circulations (Fig. 10a-d).

## 6 Summary and conclusions

This paper is a contribution to the understanding of blocking onset and decay in the Southern Hemisphere, from the analysis of atmospheric patterns. The location of blocking anticyclones is important since they have significant impacts on the weather due to atypical meteorological conditions in the South American continent. The major results concerning the climatology are:

(1) Blocking events are long-lasting and more frequent in winter (June–July–August), weaker and scarce in summer (December–January–February). The maximum activity of blocking in the winter months is followed by the spring months (September–October–November), which appears in second place in number of events and blocking days, over SEP area. The autumn months (March–April–May) come in second place regarding the number of events and blocking days, in the SAT area. A total of 48% (33%) of the events occur in winter and 6% (8%) in summer, in the SEP (SAT). The results show that blocking duration is different for each season, while blocking frequency is also different in Pacific and Atlantic blockings. The mean duration of blocking events varies between 5–8 (6–9) days over SAT (SEP) sector, although there are blockings that last more than 20 days. Furthermore, it is found that a total of 28% (13%) of the blocking events had duration longer than 10 days, over SEP (SAT);

(2) The patterns in GH composites show predominance of the Omega-type (dipole-type) blocking in SAT (SEP) sectors. Negative GH anomalies are associated with low pressure systems and depressions that move along the periphery of the blocking anticyclone. Additionally, the composites of GH anomalies in the middle troposphere give evidence that the Omega-type (dipole-type) blocking is more frequent over the SAT (SEP) sector.

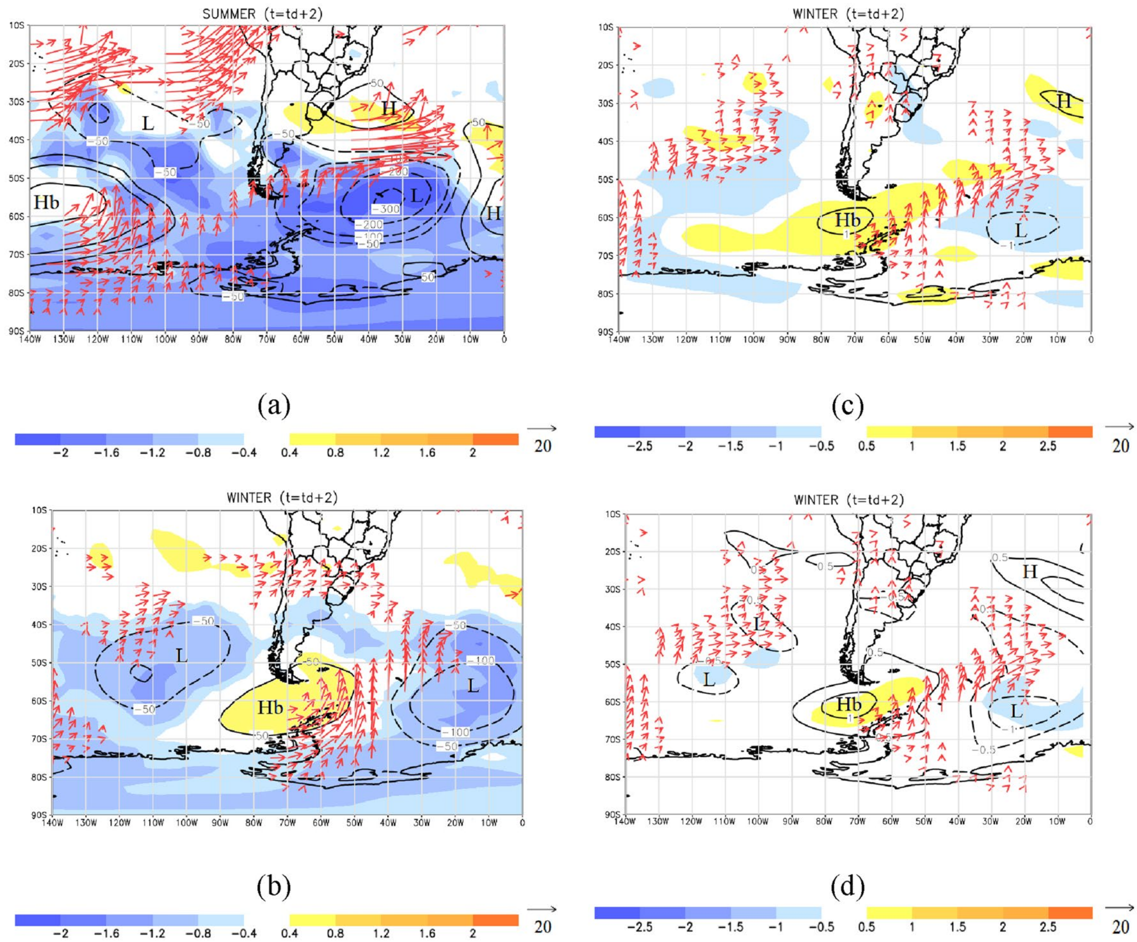


**Fig. 10** As in Fig. 6 but with respect to composites in the Southeastern Pacific

The long-lasting blocking is causally linked to the 500 hPa large amplitude of positive GH anomalies in the blocking region, resulting from the presence of a semi-stationary anomalous anticyclone. During blocking events, the large-scale atmospheric patterns are modified, especially over SEP. The main characteristics of the troposphere in blockings established in SAT and SEP are:

(1) Two days before onset ([t = to-2]), there is an increase in PV, which generates positive anomalies on the northeast (inside) of the blocking region, in SAT (SEP). It is worth noting that GH anomalies at 500 hPa show up in phase with PV anomalies of the same sign at 200 hPa. Furthermore, areas with positive RV anomalies are found in the blocking region, confirming the presence of an extensive anomalous anticyclonic circulation;

(2) On onset day ([t = to]), the centers of positive 500 hPa GH and 200 hPa PV anomalies, located in the blocking region, are intensified and their longitudinal extension is increased. These positive PV anomalies, over the blocking region, occur due to PV incursion towards the pole, which generates a tongue called "Rossby wave breaking". When the Rossby wave breaks towards the pole and the latter lasts for several days, one can associate it with a strong blocking anticyclone (Gabriel and Peters 2008).

Centers with negative PV anomalies are found around the periphery of the anomalous anticyclone, on South America and the South Atlantic, while significant westerly and southeasterly winds are located downstream of the blocking anticyclone. Furthermore, positive RV anomalies extend from low to high tropospheric levels, confirming the equivalent barotropic condition found by Pook (1995), Marques (1996) and Mendes et al. (2005), Mendes et al. (2008)). Therefore, the presence of this condition, as well as the incursion of PV towards the pole, seems to contribute to the formation and maintenance of the blocking (Mendes et al. 2019).

(3) On decay day ([t = $t_d$]), positive GH anomalies remain on the blocking region, while negative RV and PV anomalies become more extensive and elongated in the

east–west direction. The negative RV and PV anomalies are stronger on the eastern flank of the blocking anticyclone, and extend over South America. Finally, in both sectors, blockings tend to shift eastward from decay. During this period, significant southerly winds are still observed downstream of the blocking anticyclone. Finally, on decay day ($[t=t_d]$) the blocking anticyclone (anomalous anticyclonic circulation) becomes weaker and gradually moves eastward.

(4) Two days after decay ($[t=t_d+2]$), the positive RV and PV anomalies practically disappear in the blocking region. In contrast, negative PV anomalies are observed in southern South America. It is noted also the presence of negative GH and RV anomalies associated with transient systems (depressions and extratropical cyclones), prevail around the blocking anticyclone. During blocking events, the pattern of anticyclonic circulation, associated with the blocking anticyclone, is seen from the high to the low troposphere. Furthermore, the persistence of positive RV anomalies in the area and throughout the blocking period confirms the equivalent barotropic conditions in the blocking region and adjacent areas.

**Acknowledgements** The authors express their gratitude to CAPES-PNPD for financing the project “OBTENÇÃO DOS BLOQUEIOS ATMOSFÉRICOS NO PACÍFICO E ATLÂNTICO SUL PARA A ERA HOLOCÊNICA” ["Obtaining Atmospheric Blockings in the Pacific and Southern Atlantic for the Holocene Era"]. Thanks to the editor and reviewers of the journal.

## References

Adana FJS, Colucci SJ (2005) Southern hemisphere blocking onsets associated with upper-tropospheric divergence anomalies. J Atmos Sci 62:1614–1625. https://doi.org/10.1175/JAS3421.1

Austin JF (1980) The blocking of middle latitude westerly winds by planetary waves. Q J R Meteorol Soc 106:327–350. https://doi.org/10.1002/qj.49710644807

Berbery EH, Núñez MN (1989) An observational and numerical study of blocking episodes near South America. J Clim 2(11):1352–1361. https://doi.org/10.1175/1520-0442(1989)002%3c1352:AOANSO%3e2.0.CO;2

Berckmans J et al (2013) Atmospheric blocking in a high resolution climate model: influences of mean state Orography and eddy forcing. Atmos Sci Lett 14:34–40. https://doi.org/10.1002/asl2.412

Berrisford P, Hoskins BJ, Tyrlis E (2007) Blocking and rossby wave breaking on the dynamical tropopause in the southern hemisphere. J Atmos Sci 64:2881–2898. https://doi.org/10.1175/JAS3984.1

Bluestein HB (1993) Synoptic-dynamic meteorology in midlatitudes. Oxford University Press, New York, pp 1–594

Burkhardt JP, Lupo AR (2005) The planetary and synoptic-scale interactions in a Southeast Pacific blocking episode using PV diagnostics. J Atmos Sci 62:1901–1916. https://doi.org/10.1175/JAS3440.1

Colucci SJ (1985) Explosive cyclogenesis and large-scale circulation changes: implications for atmospheric blocking. J Atmos Sci 42:2701–2717. https://doi.org/10.1175/1520-0469(1985)042%3c2701:ECALSC%3e2.0.CO;2

Colucci SJ, Alberta TL (1996) Planetary-scale climatology of explosive cyclogenesis and blocking. Mon Weather Rev 124:2509–2520. https://doi.org/10.1175/1520-0493(1996)124%3c2509:PSCOEC%3e2.0.CO;2

Dee DP et al (2011) The ERA-Interim reanalysis: configuration and performance of the data assimilation system. Q J R Meteorol Soc 137:553–597. https://doi.org/10.1002/qj.828

Drouard M, Woollings T (2018) Contrasting mechanisms of summer blocking over western Eurasia. Geophys Res Lett 45:12040–12048. https://doi.org/10.1029/2018GL079894

Drouard M, Rivière G, Arbogast P (2013) The North Atlantic oscillation response to large-scale atmospheric anomalies in the northeastern Pacific. J Atmos Sci 70:2854–2874. https://doi.org/10.1175/jas-d-12-0351.1

Drouard M et al (2021) Dynamical differences between short and long blocks in the Northern Hemisphere. J Geophys Res Atmos 2:1. https://doi.org/10.1029/2020JD034082

Frederiksen JS (1982) A unified three-dimensional instability theory of the onset of blocking and cyclogenesis. J Atmos Sci 39:969–982. https://doi.org/10.1175/1520-0469(1982)039%3c0969:AUTDIT%3e2.0.CO;2

Frederiksen JS (1983) A unified three-dimensional instability theory of the onset of blocking and cyclogenesis: II. Teleconnection patterns. J Atmos Sci 40:2593–2609. https://doi.org/10.1175/1520-0469(1983)040%3c2593:AUTDIT%3e2.0.CO;2

Gabriel A, Peters D (2008) A diagnostic study of different types of Rossby events in the northern extratropics. J Meteorol Soc Japan 86(5):613–631. https://doi.org/10.2151/jmsj.86.613

Hansen AR, Chen T (1982) A spectral energetics analysis of atmospheric blocking. Mon Weather Rev 110(9):1146–1165

Hansen J et al (1983) Efficient three-dimensional global models for climate studies: models I and II. Mon Weather Rev 111:609–662

Hitchman MH, Huesmann AS (2007) A seasonal climatology of rossby wave breaking in the 320–2000-K layer. J Atmos Sci 64:1922–1940. https://doi.org/10.1175/JAS3927.1

Hoskins BJ, Mcintyre ME, Robertson AW (1985) On the use and significance of isentropic potential vorticity maps. Q J R Meteorol Soc 111:877–946. https://doi.org/10.1002/qj.49711147002

Iwabe CMN (2008) Intrusão estratosférica associada com ciclogêneses na costa do sul do Brasil: uma análise utilizando o conceito de vorticidade potencial. Dissertação de Mestrado em Meteorologia, Instituto de Astronomia, Geofísica e Ciências Atmosféricas IAGUSP, p. 1–106 (in Portuguese).

Karoly DJ (1983) Atmospheric teleconnections, forced planetary waves and blocking. Aust Meteorol Mag 31(1):51–56

Kayano MT (1999) Southeastern Pacific blocking episodes and their effect on South American weather. Meteorol Atmos Phys 69:145–155. https://doi.org/10.1007/BF01030418

Knox JL, Hay JE (1984) Blocking signatures in the Northern Hemisphere: rationale and identification. Atmos Ocean 221(1):36–47. https://doi.org/10.1080/07055900.1984.9649183

Lejenas H (1984) Characteristics of southern hemisphere blocking as determined from a long time series of observational data. Q J R Meteorol Soc 110:967–979

Lejenas H, Oakland H (1983) Characteristics of Northern Hemisphere blocking as determined from a long time series of observational data. Tellus 35:350–362

Luo D (2005) A barotropic envelope Rossby soliton model for block-eddy interaction, part I: effect of topography. J Atmos Sci 62:5–21

Luo D et al (2014) A nonlinear multiscale interaction model for atmospheric blocking: the eddy-blocking matching mechanism.

Q J R Meteorol Soc 140:1785–1808. https://doi.org/10.1002/qj.2337

Lupo AR et al (2019) Changes in global blocking character in recent decades. Atmosphere 10:92. https://doi.org/10.3390/atmos10020092

Marques RFC, Rao VB (1999) A Diagnosis of a long-lasting blocking event over the Southeast Pacific Ocean. Mon Weather Rev 127:1761–1776. https://doi.org/10.1175/1520-0493(1999)127%3c1761:ADOALL%3e2.0

Marques RFC, Rao VB (2000) A Interannual variations of blocking in the Southern Hemisphere and their energetic. J Geophys Res 105:4625–4636. https://doi.org/10.1029/1999JD901066

Marques RFC (1996) Bloqueio Atmosférico no Hemisfério Sul. São José dos Campos. Thesis (PhD.). São José dos Campos, INPE-6742-TDI/632, p. 1–158 (in Portuguese) http://marte3.sid.inpe.br/col/sid.inpe.br/iris@1905/2005/07.29.05.23/doc/publicacao.pdf

Mendes MCD, Cavalcanti IFA (2014) The relationship between the Antarctic oscillation and blocking events over the South Pacific and Atlantic Oceans. Int J Climatol 34:529–544. https://doi.org/10.1002/joc.3729

Mendes MCD et al (2005) Bloqueios atmosféricos de 1960 a 2000 sobre o Oceano Pacífico Sul: impactos climáticos e mecanismos físicos associados. Rev Bras Meteorol 20:175–190 ((**in Portuguese**))

Mendes D, Souza EP, Trigo IF, Miranda PMA (2007) On precursors of south american cyclogenesis. Tellus A 59(1):114–121. https://doi.org/10.1111/j.1600-0870.2006.00215.x

Mendes MCD et al (2008) Blocking episodes in the southern hemisphere: impact on the climate of adjacent continental areas. Pure Appl Geophys (printed Ed) 165:1–22. https://doi.org/10.1007/s00024-008-0409-4

Mendes MCD, Silva Aragão MR, Correia MF (2019) Atmospheric blockings in the southeastern pacific and south atlantic oceans: synoptic-dynamics and thermodynamic characteristics. Anuário Do Inst Geociências 42:309–324. https://doi.org/10.11137/2019_2_309_324

Mendes MCD, Cavalcanti IFA, Herdies DL (2012) Southern hemisphere atmospheric blocking diagnostic by ECMWF and NCEP/NCAR data. Rev Bras Meteorol 27: 263–271. https://www.scielo.br/pdf/rbmet/v27n3/a01v27n3.pdf

Mendes MC (2007) Bloqueios Atmosféricos sobre o Hemisfério Sul: Diagnóstico, Impacto Climático e Mecanismos físicos associados**.** Thesis (PhD). University of Lisbon, p 1–250 (in Portuguese)

Mo KC (1983) Persistent anomalies of the Southern hemisphere circulation. In preprints from the first international conference on Southern Hemisphere Meteorology. São José dos Campos. American Meteorological Society, p. 70–72

Mullen SL (1987) Transient eddy forcing and blocking flows. J Atmos Sci 44:3–22. https://doi.org/10.1175/15200469(1987)044%3c0003:TEFOBF%3e2.0.CO;2

Nakamura N, Huang CSY (2018) Atmospheric blocking as a traffic jam in the jet stream. Science 361:42–47. https://doi.org/10.1126/science.aato721

Nakamura H, Nakamura M, Anderson JLA (1997) The role of high and low frequency dynamics in blocking formation. Mon Weather Rev 125:2074–2093. https://doi.org/10.1175/1520-0493(1997)125%3c2074:TROHAL%3e2.0.CO;2

Pelly JL, Hoskins BJ (2003) A new perspective on blocking. J Atmos Sci 60:743–755. https://doi.org/10.1175/15200469(2003)060%3c0743:ANPOB%3e2.0.CO;2

Pelly JR (2001) The predictability atmospheric blocking. Thesis (PhD). University of Reading, p. 1–207

Pezzi LP, Cavalcanti IFA (1994) O jato subtropical sobre a América do Sul no período de 1980 a 1989, Anais VIII of the Brazilian Congress of Meteorology / II Latin American and Iberian Meteorological Congress, **2**, p. 148–151 (in Portuguese)

Pfahl S et al (2015) Importance of latent heat release in ascending air streams for atmospheric blocking. Nat Geosci 08:610–614. https://doi.org/10.3929/ethz-a-010690671

Pook MJ (1995) Atmospheric blocking in the Australasian region in the Southern Hemisphere winter. Thesis (PhD). University of Tasmania, Hobart, Tasmania, Australia, p. 168. https://eprints.utas.edu.au/22435/1/Pook.pdf

Renwick JA (1998) ENSO-related variability in the frequency of South Pacific blocking. Mon Weather Rev 126:3117–3123. https://doi.org/10.1175/15200493(1998)126%3c3117:ERVITF%3e2.0.CO;2

Renwick JA (2005) Persistent positive anomalies in the Southern hemisphere circulation. Mon Weather Rev 133:977–988. https://doi.org/10.1175/MWR2900.1

Renwick JA, Revell MJ (1999) Blocking over the South Pacific and Rossby wave propagation. Mon Weather Rev 127:2233–2247

Rex DF (1950a) Blocking action in the middle troposphere and its effects upon regional climate I—An aerological study of blocking action. Tellus A 2:196–211. https://doi.org/10.1111/j.2153-3490.1950.tb00331.x

Rex DF (1950b) Blocking action in the middle troposphere and its effects upon regional climate II-The climatology of blocking action. Tellus A 2:275–301. https://doi.org/10.1111/j.2153-3490.1950.tb00339.x

Rodrigues R, Woollings T (2017) Impact of atmospheric blocking on South America in austral summer. J Clim 30:1821–1837. https://doi.org/10.1175/JCLI-D-16-0493.1

Röthlisberger M, Martius O (2019) Quantifying the local effect of northern hemisphere atmospheric blocks on the persistence of summer hot and dry spells. Geophys Res Lett 46:10101–10111. https://doi.org/10.1029/2019gl083745

Ruthlant J, Fuenzalida H (1991) Synoptic aspects of the central Chile rainfall variability associated with the Southern Oscillation. Int J Climatol 11:63–76. https://doi.org/10.1002/joc.3370110105

Schwierz C, Croci-Maspoli M, Davies H (2004) Perspicacious indicators of atmospheric blocking. Geophys Res Lett. https://doi.org/10.1029/2003GL019341

Shutts GJ (1983) The propagation of eddies in diffluent jet streams: Eddy vorticity forcing of blocking flow fields. Q J R Meteorol Soc 109:737–761. https://doi.org/10.1002/qj.49710946204

Simmons AJ, Wallace JM, Branstator GW (1983) Barotropic wave propagation and instability, and atmospheric teleconnection patterns. J Atmos Sci 40(6):1363–1392. https://doi.org/10.1175/1520-0469(1983)040%3c1363:BWPAIA%3e2.0.CO;2

Sinclair MRA (1996) Climatology of anticyclones and blocking for the Southern hemisphere. Mon Weather Rev 124:245–263. https://doi.org/10.1175/1520-0493(1996)124%3c0245:ACOAAB%3e2.0.CO;2

Sprenger M, Wernli H, Bourqui M (2007) Stratosphere–troposphere exchange and its relation to potential vorticity streamers and cutoffs. J Atmos Sci 64:1587–1602. https://doi.org/10.1175/JAS3911.1

Takaya K, Nakamura H (2005) Geographical dependence of upper-level blocking formation associated with intraseasonal amplification of the siberian high. J Atmos Sci 62:4441–4449. https://doi.org/10.1175/JAS3628.1

Taljaard JJ (1972) Synoptic meteorology of the southern hemisphere. In: Newton CW (ed) Meteorology of the Southern hemisphere. Meteorological monographs. American Meteorological Society, Boston. https://doi.org/10.1007/978-1-935704-33-1_8

Tibaldi S, Molteni F (1990) On the operational predictability of blocking. Tellus A 42(1):343–365. https://doi.org/10.1034/j.1600-0870.1990.to1-2-00003.x

Tibaldi S et al (1994) Northern and Southern hemisphere seasonal variability of blocking frequency and predictability. Mon Weather Rev 122:1971–2003. https://doi.org/10.1175/1520-0493(1994)122%3c1971:NASHSV%3e2.0.CO;2

Treidl RA, Birch EC, Sajecki P (1981) Blocking action in the Northern Hemisphere: a climatological study. Atmos Ocean 19:1–23. https://doi.org/10.1080/07055900.1981.9649096

Trenberth KE, Swanson GS (1983) Blocking and persistent anomalies in the Southern Hemisphere. In Preprints from the First International Conference on Southern Hemisphere Meteorology. São José dos Campos. American Meteorological Society, p 73–76

Trenberth KE, Mo KC (1985) Blocking in the southern hemisphere. Mon Weather Rev 113:3–21

Trigo RM et al (2004) Climate impact of the European winter blocking episodes from the NCEP/NCAR Reanalyses. Clim Dyn 23:17–28. https://doi.org/10.1007/s00382-004-0410-4

Wiedenmann JM et al (2002) The climatology of blocking anticyclones for the Northern and Southern Hemisphere block intensity as a diagnostic. J Clim 15:3459–3473. https://doi.org/10.1175/1520-0442(2002)015%3c3459:TCOBAF%3e2.0.CO;2

Woollings JM et al (2018) Blocking and its response to climate change. Curr Clim Change Rep 4:287–300. https://doi.org/10.1007/s40641-018-0108-z

Wright AD (1974) Blocking action in the Australian region Australia Bureau of Meteorology. Tech Rep 10:27